Thermodynamics and Structure of Neptunium(V) Complexes with Formate. Spectroscopic and Theoretical Study

Martin M. Maiwald,* Kathy Dardenne, Jörg Rothe, Andrej Skerencak-Frech, and Petra J. Panak

ABSTRACT: The temperature and ionic strength dependences of the complex formation of NpO_2^+ with formate in aqueous solution are studied by absorption spectroscopy (I_m = 0.5−4.0 mol kg^{-1}, T = 20−85 °C, $[Form^-]_{total}$ = 0−0.65 mol kg^{-1}), extended X ray absorption fine structure spectroscopy (EXAFS) and quantum chemical methods. The complex stoichiometry and the thermodynamic functions of the complexation reactions are determined by peak deconvolution of the absorption spectra and slope analyses. Besides the solvated NpO_2^+ ion, two NpO_2^+ formate species ($NpO_2(Form)_n^{1-n}$; n = 1, 2) are identified. Application of the law of mass action yields the temperature dependent conditional stability constants log $\beta'_n(T)$ at a given ionic strength. These data are extrapolated to IUPAC reference state conditions (I_m = 0) using the specific ion interaction theory (SIT). The results show, that log β^0_1(20 °C) = 0.67 ± 0.04 decreases by approximately 0.1 logarithmic units with increasing temperature, log β^0_2(20 °C) = 0.11 ± 0.11 increases by about 0.2 logarithmic units. The temperature dependence of the log $\beta^0_n(T)$ values is modeled with the integrated Van't Hoff equation yielding the standard reaction enthalpy Δ_rH^0 and entropy Δ_rS^0 of the complexation reactions. The results show that the formation of NpO_2(Form) is exothermic ($\Delta_rH^0_1$ = −2.8 ± 0.9 kJ mol^{-1}) whereas the formation of $NpO_2(Form)_2^-$ is endothermic ($\Delta_rH^0_2$ = 6.7 ± 4.1 kJ mol^{-1}). Furthermore, the binary ion−ion interaction coefficients $\varepsilon_T(i,k)$ of the formed complexes are determined in $NaClO_4$ and NaCl media as a function of the temperature. The coordination mode of formate toward the metal ion is investigated by EXAFS spectroscopy and quantum chemical calculations. A coordination of the ligand via only one O atom of formate to the metal ion is identified.

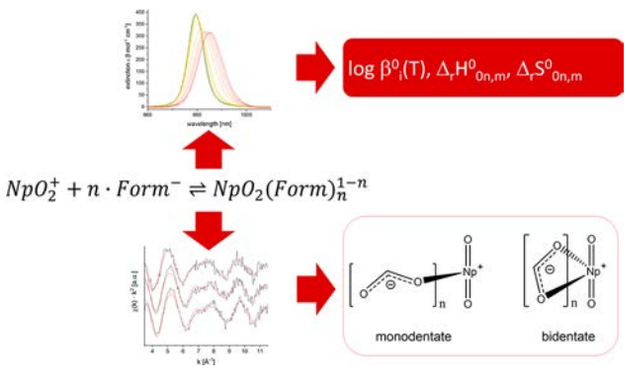

1. INTRODUCTION

The (geo)chemical behavior of actinides is of high importance for the safe disposal of highly active nuclear waste in deep geological formations.[1,2] Due to the long half lives of the trans uranium element plutonium and the minor actinides (Np, Am) these radionuclides determine the long term radiotoxicity of the nuclear waste and are of particular interest for the safety case of a nuclear waste repository.

The intrusion of water into the repository is one of the most important incident scenarios.[1] Natural organic and inorganic ligands may get into contact with the stored radioelements and influence the geochemical behavior of the actinides due to complexation reactions in the aqueous phase. Thus, different processes affecting the solubility and migration behavior of the actinides in the near and far field of a nuclear waste repository have to be considered.[3,4] For a comprehensive modeling of the migration behavior of the actinides thermodynamic data of relevant processes including standard state stability constants (log β^0_n), standard reaction enthalpies (Δ_rH^0) and entropies (Δ_rS^0) are required.

Within the thermodynamic stability field of water, the early actinides U−Am exist in the oxidation states of +III to +VI depending on the redox properties of the surrounding environment.[5,6] The An(V) ions are in general highly soluble in water whereby Np(V) is the thermodynamically most stable species among the An(V) ions. Thus, the Np(V) ion serves as analogue for An(V).

Natural clay rock formations as host rock formations for a long term high level nuclear waste repository are investigated in several European countries.[7−10] In this context, dissolved organic compounds (DOC) which are present in the pore waters of clay rock formations are of particular interest with respect to the aqueous speciation and migration of actinides. The DOC are sources for naturally occurring organic ligands and low molecular weight organic compounds (LMWOC) like formate, acetate, or propionate make up large fractions of the total DOC (i.e., Callovo Oxfordian (COX), 88% LMWOC; Opalinus Clay (OPA), 36% LMWOC).[11−14]

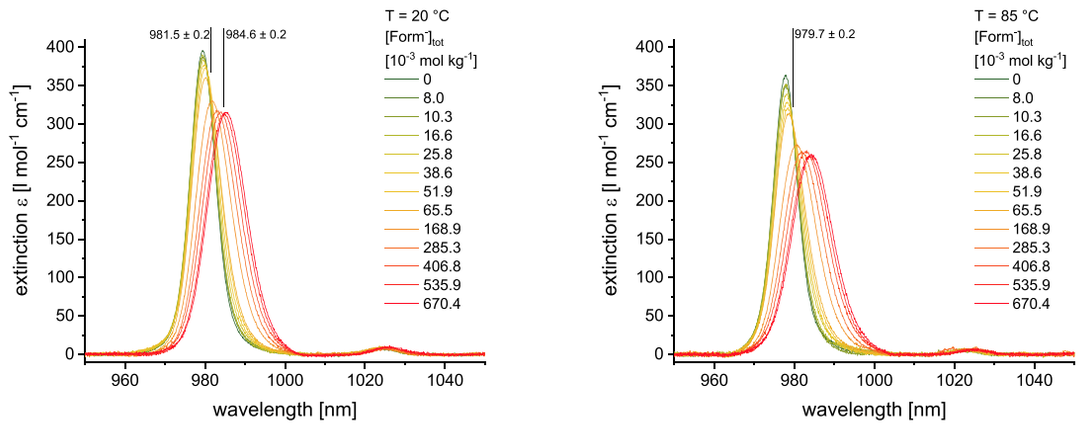

Figure 1. Absorption spectra of Np(V) as a function of the total formate concentration $[Form^-]_{total}$ at T = 20 °C (left) and T = 85 °C (right) and I_m = 4.0 mol kg^{-1} $NaClO_4$.

The present work focuses on the complexation of Np(V) with formate to gain more information on the complexation of pentavalent actinides with simple monocarboxylic acids. The complexation is studied by absorption spectroscopy in the near IR region as a function of the temperature (T = 20−85 °C), the ionic strength (I_m = 0.5−4 mol kg^{-1} $NaClO_4$ or NaCl) and the ligand concentration. Modeling the experimental data with the specific ion interaction theory (SIT) and the integrated Van't Hoff equation yields the temperature dependent standard state stability constants (log $\beta^0_n(T)$) and the thermodynamic functions $\Delta_r H^0$ and $\Delta_r S^0$ of the related complexation reactions. Furthermore, the application of the SIT yields the binary ion−ion interaction parameters $\varepsilon_T(i,k)$ of the Np(V) formate complexes with the background electrolytes NaCl and $NaClO_4$. This study is completed by EXAFS measurements and quantum chemical calculations yielding information on the structure of the formed complexes.

In the literature no data for the complex formation of Np(V) with formate is available and only a few studies on the complexation of Np(V) with acetate and propionate were performed.[15−20] Thus, the present study provides additional thermodynamic data for the complexation of Np(V) with simple water soluble monocarboxylic acids. Furthermore, structural parameters of the formed complexes determined by EXAFS spectroscopy and quantum chemical calculations give a deeper insight into the coordination chemistry of Np(V) on a molecular level.

2. EXPERIMENTAL SECTION

Caution! *^{237}Np is a radioactive nuclide emitting α particles. It must be handled with caution in laboratories appropriate for handling transuranic elements to avoid health risks caused by radiation exposure or incorporation.*

All solutions were prepared on the molal concentration scale (mol (kg H_2O)$^{-1}$; index "*m*") to avoid changes of the concentration due to changes in temperature and/or ionic strength. All chemicals were analytical grade or higher and purchased from Merck Millipore. Ultrapure water (Milli Q academic, Millipore) was used for sample preparation.

2.1. Absorption Spectroscopy. For the speciation studies by absorption spectroscopy the initial Np(V) concentration of the samples was set to 2.7 × 10^{-4} mol kg^{-1} by dilution of an aqueous isotope pure 5.93 × 10^{-2} mol kg^{-1} ^{237}Np(V) stock solution provided by the Institute for Nuclear Waste Disposal (INE) at the Karlsruhe Institute of Technology (KIT). The proton concentration of the ^{237}Np(V) stock solution was $[HClO_4]_{stock}$ = 2.9 × 10^{-4} mol kg^{-1}. Details on the preparation of the stock solution are given in the literature.[21] The oxidation state of the Np stock solution and its concentration were confirmed by absorption spectroscopy and solvent extraction techniques.[22] The total proton concentration of the samples was set to $[H^+]_{total}$ = 2.7 × 10^{-5} mol kg^{-1} using a 0.1 mol kg^{-1} $HClO_4$. The complexation reaction was studied as a function of the total formate concentration ($[Form^-]_{total}$ = 0−0.65 mol kg^{-1}) at a fixed ionic strength (I_m = 4.0 mol kg^{-1} $NaClO_4$). The formate concentration was increased by addition of aliquots of a solution with $[Form^-]_{total}$ = 4.0 mol kg^{-1} and $[H]^+_{total}$ = 2.7 × 10^{-5} mol kg^{-1}. The ionic strength dependence of the complex formation was investigated at a fixed ligand concentration ($[Form^-]_{total}$ = 0.5 mol kg^{-1}) at increasing concentrations of the background electrolytes ($NaClO_4$ or NaCl) between I_m = 0.5 and 4.0 mol kg^{-1}. The concentration of $NaClO_4$ was adjusted by addition of aliquots of an aqueous 13.1 mol kg^{-1} $NaClO_4$ solution. The NaCl ionic strength was increased by addition of solid NaCl to the samples. All measurements were performed in the temperature range of 20 to 85 °C. The absorption spectroscopic measurements of the Np(V) samples in the near IR region were performed on a Varian Cary 5G UV/vis/NIR spectrophotometer. The temperature of the sample holder was controlled using a Lauda Eco E100 thermostatic system. The cuvettes (quartz glass with airtight screw caps, 1 cm path length, Hellma Analytics) were pre equilibrated at the different temperatures in a custom made copper sample holder. The samples were equilibrated for 15 min at each temperature step to ensure chemical equilibrium before measurement. Absorption spectra were recorded with data intervals of 0.1 nm, a scan rate of 60 nm min^{-1} (average time: 0.1 s), and a slit width of 0.7 nm in double beam mode.

2.2. EXAFS Spectroscopy. For the EXAFS measurements, an initial Np(V) concentration of 3.5 × 10^{-3} mol kg^{-1} was used. The measurements were performed using two different total proton concentrations ($[H^+]_{total}$ = 1.8 × 10^{-5} and 3.4 × 10^{-2} mol kg^{-1}) at a fixed ionic strength (I_m($NaClO_4$/NaForm) = 3.9 mol kg^{-1}) and formate concentration ($[Form^-]_{total}$ = 0.6 mol kg^{-1}). The proton concentration was varied using a 6 mol kg^{-1} $HClO_4$ solution.

Np L_3 EXAFS spectra were measured in fluorescence mode at an angle of 90° using a four element Si SDD Vortex (SIINT) and an additional one element Si Vortex 60EX SDD (SIINT) fluorescence detector at an angle of 60°. All measurements were performed at the INE Beamline of the *Karlsruhe Research Accelerator* (KARA, Karlsruhe, Germany).[23−25] The beamline was equipped with a double crystal monochromator (DCM) and a collimating and focusing mirror system (Rh coated silicon mirrors). In the present study, a Ge(422) crystal pair was used in the DCM. The DCM was detuned in the middle of the scan range to 70% peak flux intensity. The incident X ray intensity I_0 was measured with an Ar filled ionization chamber at ambient pressure. Within the EXAFS range, the measurements were performed at equidistant k steps, and the integration time was increased continuously with a $\sqrt[3]{2}$ progression.

Measurements were performed at 25 °C. The data were evaluated with the software packages EXAFSPAK, Athena 0.8.056, and Artemis 0.8.012.[26−28] Theoretical scattering path and amplitudes were calculated with FEFF8.40 using the crystal structures of UO_2−acetate and −succinate.[29−31] Hereby, the U atom was replaced by Np. In all cases, the k^2 and k^3 weighted raw EXAFS spectra are evaluated.

The EXAFS samples were analyzed by vis/NIR spectroscopy and solvent extraction techniques to ensure that no redox processes occurred during the EXAFS measurements.[22]

2.3. Quantum Chemical Calculations. Quantum chemical calculations and structure optimizations of the Np(V) formate complexes were carried out using the TURBOMOLE 7.0 program package.[32] The NpO_2(Form) and $NpO_2(Form)_2^-$ complexes with different coordination modes (monodentate vs bidentate) were optimized employing density functional theory (DFT). The BH LYP functional was chosen for its better convergence compared to other hybrid functionals.[32,33] For all N, C, and H atoms basis sets of triple ζ basis quality (def TZVP) were used and were treated at the all electron level. The metal ion was represented by a 60 electron core pseudopotential (Np, ECP60MWB) with corresponding basis sets.[34] For all systems, the triplet spin state was used with two unpaired f electrons. The gas phase energies E_g were computed on MP2 level taking into account thermodynamic corrections ($E_{vib} = E_{zp} + H_0 - TS$, E_{zp} being the zero point energy) and solvation energies E_{solv} (using COSMO) to obtain a theoretical approximation of the Gibbs free energies $G = E_g + E_{vib} + E_{solv}$.[35−37] Additionally, due to the ionic charge of the Np(V) complexes, a full second hydration shell was added to avoid the charge of the complexes to contact the COSMO cavity.

3. RESULTS AND DISCUSSION

3.1. Vis/NIR Spectroscopy. In Figure 1 the absorption spectra of Np(V) are displayed as a function of $[Form^-]_{total}$ at T = 20 and 85 °C (I_m = 4.0 mol kg^{-1} $NaClO_4$). The absorption band of the Np(V) aquo ion at 20 °C is located at 979.6 ± 0.1 nm with a molar extinction coefficient of $\varepsilon_{20\ °C}$ = 394 ± 5 l mol^{-1} cm^{-1} (Figure 1 (left)). This value is in excellent agreement with the literature, where the spectroscopic properties of Np(V) were also studied at comparable ionic strength conditions.[15,38] Compared to I_m < 0.5 mol kg^{-1}, the absorption band of the solvated Np(V) ion is shifted by 0.6 nm toward shorter wavelengths.[39,40] With increasing formate concentration the absorption band shifts bathochromically, displaying two isosbestic points at 981.5 ± 0.2 and 984.6 ± 0.2 nm. This indicates the formation of two different Np(V) formate complexes. The bathochromic shift is accompanied by a broadening of the full width at half maximum (fwhm) from 7.4 to 11.6 nm. At T = 85 °C (see Figure 1 (right)) the absorption band of the Np(V) aquo ion is located at 977.8 ± 0.1 nm. Thus, the spectrum is hypsochromically shifted by 1.8 nm compared to 20 °C. The temperature induced blue shift is in accordance with the literature.[15,38,41,42] The fwhm of the Np(V) aquo ion is unaffected by the temperature whereas the molar extinction coefficient decreases to $\varepsilon_{85\ °C}$ = 359 ± 7 l mol^{-1} cm^{-1}. The bathochromic shift of the absorption band with increasing formate concentration is slightly more pronounced at elevated temperatures and the fwhm increases from 7.2 to 12.0 nm, indicating a fostered formation of $NpO_2(Form)_n^{1-n}$ complexes. At 85 °C, only one isosbestic point is observed at 979.7 ± 0.2 nm. This point is shifted hypsochromically by 1.8 nm compared to 20 °C. Thus, the temperature induced shift of the isosbestic point is identical to the shift of the absorption band of the solvated Np(V) ion. This shows that the hypsochromic shift with increasing temperature is affecting the Np(V) absorption in general and does not depend on the speciation in the solution.

The temperature induced hypsochromic shift of the absorption band of Np(V) is contrary to the bathochromic shift of the spectra resulting from the complexation of Np(V) with formate. Therefore, each series of spectra has to be evaluated separately and single component spectra have to be determined for all studied temperatures and ionic strength conditions.

3.2. Peak Deconvolution and Single Component Spectra. The single component spectra of the complex species NpO_2(Form) and $NpO_2(Form)_2^-$ are derived by subtractive peak deconvolution using the spectrum of the Np(V) aquo ion recorded at each temperature and ionic strength condition. Details on this procedure are given in the literature.[43] The obtained single component spectra are identical in NaCl and $NaClO_4$ media at equal ionic strength and temperature and are displayed in Figure 2 for 20 and 85

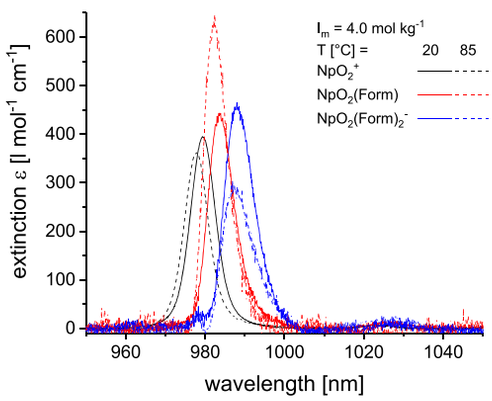

Figure 2. Single component spectra of the Np(V) aquo ion and the $NpO_2(Form)_n^{1-n}$ (n = 1, 2) complexes at 20 and 85 °C and I_m = 4.0 mol kg^{-1} $NaClO_4$.

°C at I_m = 4.0 mol kg^{-1}. At 20 °C, the absorption spectrum of NpO_2(Form) is located at 983.8 ± 0.2 nm ($\varepsilon_{20\ °C}$ = 434 ± 22 L mol^{-1} cm^{-1}) and that of $NpO_2(Form)_2^-$ at 988.0 ± 0.2 nm ($\varepsilon_{20\ °C}$ = 453 ± 23 L mol^{-1} cm^{-1}). Thus, a bathochromic shift of about 4.2 nm is induced by each coordinating ligand molecule compared to the Np(V) aquo ion at 20 °C. With increasing temperature the absorption band of the Np(V) aquo ion and the Np(V) formate complexes are shifted hypso chromically. At 85 °C the absorption band of the Np(V) aquo ion is located at 977.8 ± 0.1 nm which corresponds to a hypsochromic shift of 1.8 nm compared to 20 °C. The fwhm is unaffected by the temperature and the molar extinction coefficient decreases to $\varepsilon_{85\ °C}$ = 359 ± 7 l mol^{-1} cm^{-1}. The spectrum of NpO_2(Form) is shifted to 982.3 ± 0.2 nm ($\varepsilon_{85\ °C}$ = 647 ± 32 l mol^{-1} cm^{-1}) and that of $NpO_2(Form)_2^-$ to 986.8 ± 0.2 nm ($\varepsilon_{85\ °C}$ = 304 ± 15 l mol^{-1} cm^{-1}). For both complex species only minor effects of the temperature on the fwhm are observed. The spectroscopic properties of the formed complexes are summarized in Table 1 for 20 and 85 °C and I_m = 4.0 mol kg^{-1} $NaClO_4$.

Comparison of the hypsochromic shift of the single component spectra of the different complex species with the Np(V) aquo ion reveals that the temperature induced hypsochromic shift is weaker for the complexed Np(V) ion. The spectrum of the 1:1 complex shifts by 1.5 nm to shorter wavelengths, while the spectrum of the 1:2 complex shifts only by 1.2 nm in the studied temperature range.

Table 1. Spectroscopic Parameters of the Single Component Spectra of the the Np(V) Aquo Ion and the $NpO_2(L)_n^{1-n}$ Complexes (L = $Form^-$, Ac^-, $Prop^-$, n = 1, 2) at 20 and 85 °C and I_m = 4.0 mol kg^{-1} $NaClO_4$[15,16]

T [°C]	species	λ_{max} [nm]	ε [l mol^{-1} cm^{-1}]	fwhm [nm]	lit.
20	NpO_2^+	979.6 ± 0.1	392 ± 7	7.3 ± 0.4	p.w.[a]
	$NpO_2(Form)$	983.8 ± 0.2	434 ± 22	7.7 ± 0.4	p.w.
	$NpO_2(Form)_2^-$	988.0 ± 0.2	453 ± 23	8.5 ± 0.4	p.w.
	$NpO_2(Ac)$	984.2 ± 0.2	192 ± 9	8.9 ± 0.4	15
	$NpO_2(Ac)_2^-$	989.6 ± 0.2	80 ± 4	8.6 ± 0.4	15
	$NpO_2(Prop)$	~ 984	180 ± 10		16
85	NpO_2^+	977.8 ± 0.1	359 ± 9	7.2 ± 0.4	p.w.
	$NpO_2(Form)$	982.3 ± 0.2	647 ± 32	6.8 ± 0.3	p.w.
	$NpO_2(Form)_2^-$	986.8 ± 0.2	304 ± 15	8.6 ± 0.4	p.w.
	$NpO_2(Ac)$	982.6 ± 0.2	176 ± 9	9.9 ± 0.5	15
	$NpO_2(Ac)_2^-$	988.3 ± 0.2	89 ± 5	10.3 ± 0.5	15

[a]p.w. = present work.

It is known from the literature that the temperature and the ionic strength significantly affect the absorption of the Np(V) ion in aqueous solution.[38,41,44] The hypsochromic shift is explained by different theories. Besides the thermal expansion of the complex size, which results in changes of the ligand field and thus affects the absorption of the Np(V) ion, changes in the solvation of the Np(V) ion and solvatochromic effects are discussed. Furthermore, the temperature and ionic strength affect the physical properties of water (e.g., dielectric constant, refractive index, polarity) which may also result in changes of the absorption properties of the Np(V) ion. Due to the temperature and ionic strength dependency of the absorption bands, each series of spectra has to be treated separately using the specific single component spectra at the given experimental condition.

Additionally, in Table 1 the spectroscopic parameters of $NpO_2(Form)_n^{1-n}$ (n = 1, 2) are compared to those of $NpO_2(Ac)_n^{1-n}$ (n = 1, 2) and $NpO_2(Prop)$.[15,16]

At room temperature, the positions of the absorption bands of the $NpO_2(Form)_n^{1-n}$ complexes are in good agreement with those of the respective $NpO_2(Ac)_n^{1-n}$ (n = 1, 2) and $NpO_2(Prop)$ species given in the literature.[15,16] The similar shift of the absorption bands of the different complexes results from the similar binding strength of the monocarboxylic ligands leading to a comparable ligand field splitting of the exited state of the Np(V) ion. Despite the similar energy gap between the ground and the exited state, however, the extinction coefficients of the formate complexes differ significantly from the extinction coefficients of the acetate or propionate species. The observed transitions in the Np(V) ion originate from intraconfiguration $5f^2$ transitions and are forbidden by Laport's rule. They become partially allowed by vibronic coupling and changes in the symmetry due to complexation of the Np(V) ion. Thus, small differences in the structure and symmetry of the complexes may cause significant differences in the transition probabilities of $NpO_2(Form)_n^{1-n}$ compared to $NpO_2(Ac)_n^{1-n}$ (n = 1, 2) and $NpO_2(Prop)$.

3.3. Species Distribution and Complex Stoichiometry. The speciation of the Np(V) formate system is derived by deconvolution of the experimental absorption spectra by principle component analysis using the single component spectra. Details on this procedure are given in the literature.[43,45] In Figure 3 the experimental (symbols) and the calculated speciation (lines, using the derived log $\beta'_n(T)$ values (see Table 3)) are displayed as a function of the equilibrium formate concentration $[Form^-]_{eq}$ at T = 20 and 85 °C and I_m = 4.0 mol kg^{-1} $NaClO_4$. With increasing $[Form^-]_{eq}$ the chemical equilibrium shifts toward the complexed Np(V) species. At 20 °C the species distribution is dominated by the $NpO_2(Form)$ complex between $[Form^-]_{eq}$ = 0.2–0.9 mol kg^{-1}. For higher $[Form^-]_{eq}$ $NpO_2(Form)_2^-$ becomes the dominant species. At 85 °C the $NpO_2(Form)$ complex is formed to a lower extend and $NpO_2(Form)_2^-$ prevails the speciation at $[Form^-]_{eq}$ > 0.4 mol kg^{-1}. The comparison of the species distributions at 20 and 85 °C shows that the speciation of the two Np(V) formate complexes is affected in different ways by the increase of the temperature. At equal ligand concentrations the molar fractions of $NpO_2(Form)$ decrease whereas the molar fractions of $NpO_2(Form)_2^-$ increase.

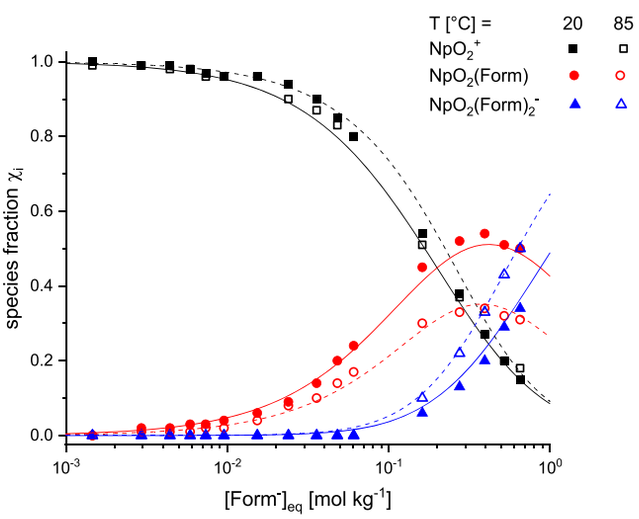

Figure 3. Experimental (symbols) and calculated (lines) species distribution of $NpO_2(Form)_n^{1-n}$ (n = 0–2) complexes as a function of $[Form^-]_{eq}$ in aqueous solution at I_m = 4.0 mol kg^{-1} $NaClO_4$. Calculations with log β'_1(20 °C) = 0.68 ± 0.18, log β'_2(20 °C) = 0.76 ± 0.12, log β'_1(85 °C) = 0.47 ± 0.21, and log β'_2(85 °C) = 0.88 ± 0.09. T = 20 (solid lines) and 85 °C (dashed lines).

For the determination of the stoichiometry of the formed complexes and validation of the single component spectra slope analyses are performed at each studied temperature. The complexation model according to eq 1 is applied:

$$NpO_2^+ + Form^- \rightleftharpoons NpO_2(Form)$$
$$NpO_2(Form) + Form^- \rightleftharpoons NpO_2(Form)_2^-$$
$$\vdots$$
$$NpO_2(Form)_{n-1}^{1-(n-1)} + Form^- \rightleftharpoons NpO_2(Form)_n^{1-n} \quad (1)$$

The slope analyses for the stepwise complex formation are performed using the logarithmic form of the law of mass action (eq 2):

$$\log K'_n = \log \frac{[NpO_2(Form)_n]^{1-n}}{[NpO_2(Form)_{n-1}]^{1-(n-1)}} - \log[Form]^-_{eq};$$
$$\beta'_n = \prod K'_n \quad (2)$$

with $[Form^-]_{eq}$ being the concentration of the free, deprotonated formate in solution at the given experimental conditions. In aqueous solution, formate is in chemical equilibrium with its protonated form (formic acid). The Henderson–Hasselbalch equation is used to calculate the free formate concentration $[Form^-]_{eq}$ at a given temperature and ionic strength according to literature procedure.[15,46] Therefore, the protonation constant as a function of the temperature and ionic strength is calculated from pK^0_a with the specific ion interaction theory and the integrated Van't Hoff equation. Details on this procedure are given in the literature.[15] The required SIT binary ion–ion interaction coefficients and the temperature dependence of the pK^0_a value are given in the NEA TDB and NIST standard reference database.[47,48]

The plots of $\log \frac{[NpO_2(Form)_n]^{1-n}}{[NpO_2(Form)_{n-1}]^{1-(n-1)}}$ vs $\log[Form]^-_{eq}$ and the linear regression analyses are displayed in Figure 4 for 20 and

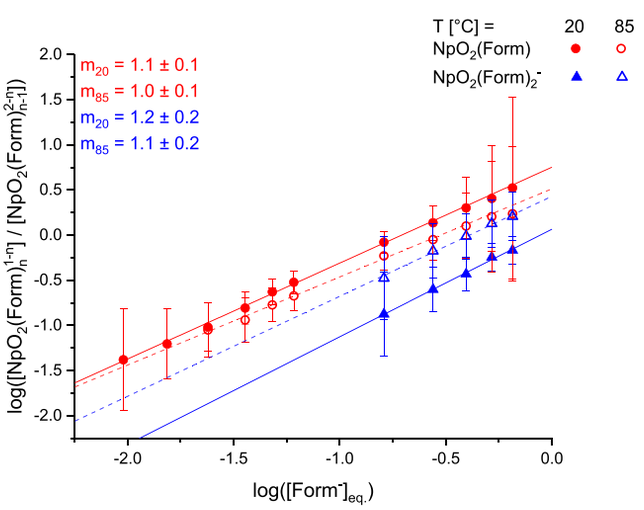

Figure 4. Linear regression analyses of log $([NpO_2(Form)_n]^{1-n}/[NpO_2(Form)_{n-1}]^{2-n})$ vs log $([Form^-]_{eq})$ according to eq 2 at 20 and 85 °C (I_m = 4.0 mol kg^{-1} $NaClO_4$).

85 °C at I_m = 4.0 mol kg^{-1}. A linear correlation of the data is observed at each studied temperature and the linear regression analyses reveal slopes between 0.9 ± 0.1 and 1.2 ± 0.2 at all experimental conditions. Thus, the formation of $NpO_2(Form)_n^{1-n}$ (n = 1, 2) is confirmed.

3.4. Thermodynamic Data. The law of mass action (eq 2) is used to calculate the log $\beta'_n(T)$ values for the formation of $NpO_2(Form)$ and $NpO_2(Form)_2^-$ at different ionic strengths and temperatures using the species distribution at a fixed ligand concentration $[Form^-]_{total}$. The species distribution as a function of the ionic strength is displayed in Figure S1 in the Supporting Information at T = 20 and 85 °C. At both temperatures, the molar fractions of the solvated Np(V) ion decrease whereas the fractions of $NpO_2(Form)$ remain constant and the fractions of $NpO_2(Form)_2^-$ increase with increasing I_m. These observations agree with the fact that increasing ionic strengths have a minor effect on the molar fractions of uncharged species.

In Figure 5 the ionic strength dependence of log $\beta'_n(T) - \Delta z^2 D$ are plotted as a function of $I_m(NaClO_4)$ according to the SIT (eq 3).[49,50]

$$\log K' - \Delta z^2 D = \log K^0 + \Delta \varepsilon I_m \quad (3)$$

A linear correlation of log $\beta'_n(T) - \Delta z^2 D$ with I_m is found for all studied temperatures and the conditional stability constants are extrapolated to I_m = 0 yielding the thermodynamic stability constants log $\beta^0_n(T)$. In Table 2, the obtained log $\beta^0_n(T)$, determined from conditional data in NaCl and $NaClO_4$ media, are summarized. At a given temperature, the log $\beta^0(T)$ values are in excellent agreement and averaged values "Ø" are calculated. With increasing temperatures log β^0_1(20 °C) = 0.67 ± 0.04 for $NpO_2(Form)$ decreases by 0.1 logarithmic units whereas log β^0_2(20 °C) = 0.11 ± 0.11 for $NpO_2(Form)_2^-$ increases by approximately 0.2.

In Figure 6, the averaged log $\beta^0_n(T)$ values are plotted as a function of the reciprocal temperature T^{-1}. The data correlate linear with T^{-1}; thus, the temperature dependence is well described by the integrated Van't Hoff equation (eq 4). Therefore, the reaction enthalpies $\Delta_r H^0_{m,n}$ and entropies $\Delta_r S^0_{m,n}$ are calculated with eq 4.

$$\log \beta^0_n(T) = \log \beta^0_n(T_0) + \frac{\Delta_r H^0_{m,n}(T_0)}{R \ln(10)}\left(\frac{1}{T_0} - \frac{1}{T}\right) \quad (4)$$

with R being the universal gas constant, T the absolute temperature in K and T_0 = 298.15 K. The Van't Hoff equation is commonly valid for small changes in the temperature of about $\Delta T \approx 80$ K, assuming $\Delta_r C^0_{m,p}$ = 0 and $\Delta_r H^0_m$ = const. Linear regression analyses according to eq 4 yield $\Delta_r H^0_{m,n}$ of the complexation reactions. $\Delta_r S^0_{n,m}$ is calculated using the Gibbs–Helmholtz equation (eq 5).

$$\Delta_r G^0_{m,n} = \Delta_r H^0_{m,n} - T \cdot \Delta_r S^0_{m,n} = -RT \ln \beta^0_n \quad (5)$$

The averaged reaction enthalpies are $\Delta_r H^0_{m,1}$ = −2.8 ± 0.9 kJ mol^{-1} and $\Delta_r H^0_{m,2}$ = 6.7 ± 4.1 kJ mol^{-1} for the formation of $NpO_2(Form)$ and $NpO_2(Form)_2^-$. The standard reaction entropies are $\Delta_r S^0_{m,1}$ = 4 ± 2 J mol^{-1} K^{-1} and $\Delta_r S^0_{m,2}$ = 27 ± 12 J mol^{-1} K^{-1}. Thus, the formation of $NpO_2(Form)$ is slightly exothermic whereas the formation of $NpO_2(Form)_2^-$ is endothermic. The $\Delta_r H^0_{m,n}$ and $\Delta_r S^0_{m,n}$ values determined in the present work are summarized in Table 3.

The integrated Van't Hoff eq (eq 4) is used to calculate the log β^0_n(25 °C) values of the formate complexes. These values are also given in Table 3. No thermodynamic stability constants for the complexation of Np(V) with formate are available in the literature. Thus, these data are compared to literature data for the complexation of Np(V) with acetate and propionate

Spectrophotometric and solvent extraction studies on the Np(V) complexation with acetate provide log β^0_1 (25 °C)

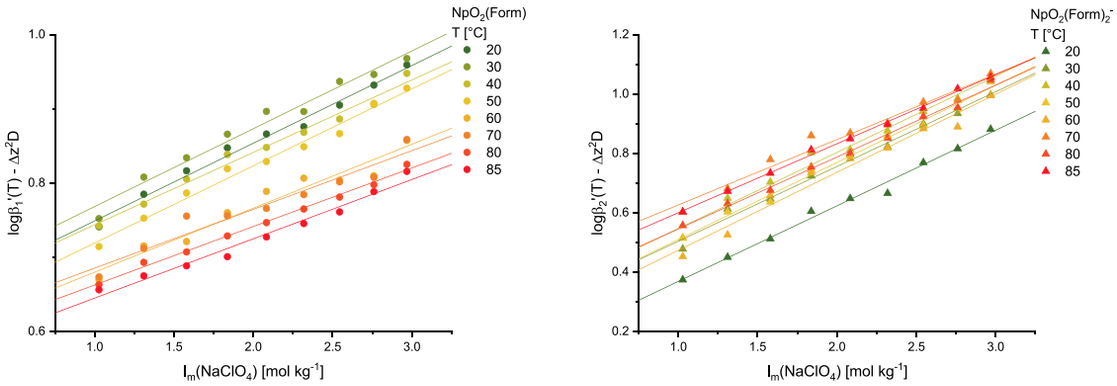

Figure 5. Ionic strength dependence of $\log \beta'_n(T) - \Delta z^2 D$ and linear fitting of the data according to the SIT for the complexation reaction $NpO_2^+ + n\text{Form}^- \rightleftharpoons NpO_2(\text{Form})_n^{1-n}$ (n = 1, 2) in $NaClO_4$.

Table 2. $\log \beta^0_n(T)$ Values for the Complexation Reaction $NpO_2^+ + n\text{Form}^- \rightleftharpoons NpO_2(\text{Form})_n^{1-n}$ (n = 1, 2), Determined from Conditional Data in $NaClO_4$ and NaCl Media and the Averaged Values as a Function of the Temperature (Ø = Averaged Values)

		T = 20 °C	T = 30 °C	T = 40 °C	T = 50 °C	T = 60 °C	T = 70 °C	T = 80 °C	T = 85 °C
$[NpO_2\text{Form})]$	NaCl	0.70 ± 0.02	0.67 ± 0.05	0.66 ± 0.06	0.61 ± 0.05	0.62 ± 0.05	0.63 ± 0.02	0.62 ± 0.06	0.58 ± 0.03
	$NaClO_4$	0.64 ± 0.03	0.66 ± 0.04	0.65 ± 0.03	0.62 ± 0.03	0.59 ± 0.05	0.61 ± 0.05	0.58 ± 0.01	0.56 ± 0.03
	Ø	0.67 ± 0.04	0.67 ± 0.07	0.65 ± 0.06	0.61 ± 0.06	0.60 ± 0.07	0.62 ± 0.05	0.60 ± 0.06	0.57 ± 0.04
$[NpO_2(\text{Form})_2]$	NaCl	0.11 ± 0.09	0.22 ± 0.08	0.20 ± 0.07	0.18 ± 0.08	0.31 ± 0.07	0.36 ± 0.06	0.32 ± 0.07	0.33 ± 0.07
	$NaClO_4$	0.11 ± 0.06	0.26 ± 0.06	0.30 ± 0.08	0.27 ± 0.07	0.24 ± 0.11	0.44 ± 0.09	0.35 ± 0.04	0.40 ± 0.06
	Ø	0.11 ± 0.11	0.24 ± 0.10	0.25 ± 0.10	0.22 ± 0.10	0.28 ± 0.13	0.40 ± 0.11	0.34 ± 0.08	0.37 ± 0.09

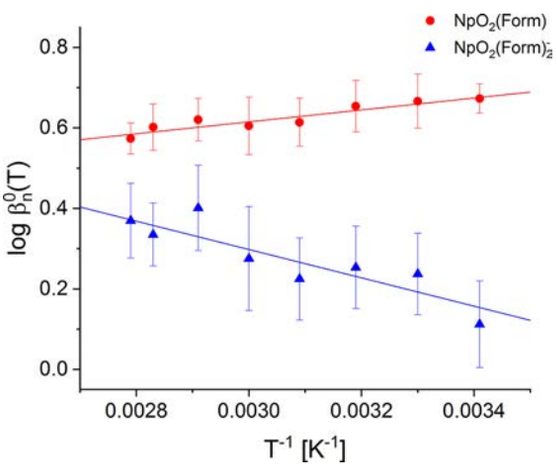

Figure 6. Plot of $\log \beta^0_n(T)$ (n = 1, 2) as a function of the reciprocal temperature and linear regression analyses according to the integrated Van't Hoff equation.

values for the 1:1 complex between 1.31 ± 0.27 and 1.46 ± 0.22.[15,19,20,51] Only in the spectrophotometric and calorimetric studies by Rao et al. is a lower $\log \beta^0_1$ (25 °C) for $NpO_2(Ac)$ of 1.05 ± 0.04 reported.[18] Nonetheless, the here obtained stability constant of $NpO_2(\text{Form})$ is by about 0.7 logarithmic units lower compared to the value of the 1:1 Np(V) acetate complex. This significant difference of the thermodynamic stability between acetate and formate was also observed for trivalent actinides.[46,52] The stability constant of $Cm(Ac)^{2+}$ was determined to $\log \beta^0_1$ (25 °C) = 3.12 ± 0.32 whereas $\log \beta^0_1$ (25 °C) of $Cm(\text{Form})^{2+}$ is 2.11 ± 0.01. Furthermore, the stability constants of the $NpO_2(L)$ complexes of formate and propionate also differ by approximately 0.6 logarithmic units. The difference between the $\log \beta^0_2$ (25 °C) values of $NpO_2(\text{Form})_2^-$ and $NpO_2(Ac)_2^-$ is even higher and equals 1.1 logarithmic units.

The difference in the complex stability of Np(V) with acetate, propionate, and formate is due to the chemical properties of the carboxylates. Although the coordinating functional group is identical for these ligands the alkyl backbone has a distinct effect on the electron density at the carboxylic group and thus on the complex stability. The +I effect of the methyl and ethyl moieties increases the electron density at the carboxylic group, resulting in higher complex stabilities. A similar trend is observed within the series of pK_a values for the corresponding acids.[48]

Due to a lack of literature data, a comparison of reaction enthalpies and entropies for the complex formation of

Table 3. Thermodynamic Data ($\log \beta^0_n$(25 °C), $\Delta_r H^0_{m,n}$, $\Delta_r S^0_{m,n}$ $\Delta\varepsilon_{0n}$) for the Formation of $NpO_2(\text{Form})_n^{1-n}$ (n = 1, 2]

electrolyte	$NpO_2(\text{Form})_n^{1-n}$	$\log \beta^0_n$(25 °C)	$\Delta_r H^0_{m,n}$ [kJ mol^{-1}]	$\Delta_r S^0_{m,n}$ [J mol^{-1}K^{-1}]	$\Delta\varepsilon_{0_i}$
$NaClO_4$	n = 1	0.68 ± 0.16	2.5 ± 1.1	4 ± 3	0.09 ± 0.04
	n = 2	0.18 ± 0.36	6.8 ± 4.5	27 ± 14	0.16 ± 0.05
NaCl	n = 1	0.65 ± 0.15	3.0 ± 1.5	3 ± 5	0.10 ± 0.05
	n = 2	0.15 ± 0.25	7.1 ± 4.6	27 ± 14	0.15 ± 0.06
Ø	n = 1	0.67 ± 0.16	2.8 ± 0.9	4 ± 2	
	n = 2	0.17 ± 0.31	6.7 ± 4.1	27 ± 12	

Table 4. Thermodynamic Functions (log β^0_n, $\Delta_r H^0_{n,m}$, $\Delta_r S^0_{n,m}$) for the Complexation of Np(V) with Formate, Acetate, and Propionate at 25 °C[a]

	method	electrolyte	log $\beta^0_{25\ °C}$	$\Delta_r H^0_{n,m}$ [kJ mol^{-1}]	$\Delta_r S^0_{n,m}$ [J mol^{-1}K^{-1}]	ref
$[NpO_2(Form)]$	sp	$NaCl/NaClO_4$	0.67 ± 0.16	2.8 ± 0.9	4 ± 2	p.w.
$[NpO_2(Form)_2]^-$	sp	$NaCl/NaClO_4$	0.17 ± 0.31	6.7 ± 4.1	27 ± 12	p.w.
$[NpO_2(Ac)]$	sp	$NaCl/NaClO_4$	1.31 ± 0.27	14.8 ± 1.6	74 ± 10	15
	sp, cal	$NaClO_4$	1.05 ± 0.04			18
	sx	$NaClO_4$	1.35			19
	sx	NaCl	1.46 ± 0.22			51
	sx	NaCl	1.30 ± 0.06[b]			20
$[NpO_2(Ac)_2]^-$	sp	$NaCl/NaClO_4$	1.33 ± 0.29	19.0 ± 2.1	89 ± 16	15
$[NpO_2(Prop)]$	sp	NaCl	1.26 ± 0.03	10.9 ± 1.2	62 ± 4	16

[a]Key: p.w. = present work, sp = spectrophotometry, sx = solvent extraction, and cal = calorimetry. [b]Calculated from literature data.

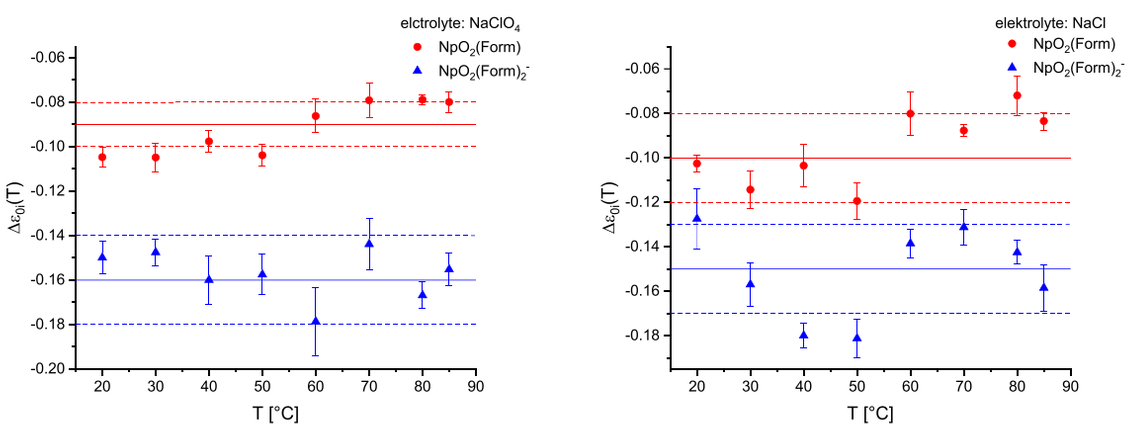

Figure 7. Stoichiometric sum of the binary ion−ion interaction coefficients $\Delta\varepsilon_{0n}$ for the complexation reaction $NpO_2^+ + n\text{Form}^- \rightleftharpoons NpO_2(Form)_n^{1-n}$ (n = 1, 2) in $NaClO_4$ (left) and NaCl (right) as a function of the temperature. The dashed lines equal the 2σ error of the mean values (solid lines).

$NpO_2(Form)_n^{1-n}$ (n = 1, 2) is not possible. Thus, the comparison is made to values of the Np(V) acetate and propionate systems (see Table 4). The formation of $NpO_2(Ac)_n^{1-n}$ (n = 1, 2) is endothermic for both complexation steps ($\Delta_r H^0_{m,1}(NpO_2(Ac))$ = 14.8 ± 1.6 kJ mol^{-1}, $\Delta_r H^0_{m,2}(NpO_2(Ac)_2^-)$ = 19.0 ± 2.1 kJ mol^{-1}) and the reactions are driven by the high gain of entropy ($\Delta_r S^0_{m,1}(NpO_2(Ac))$ = 74 ± 10 J mol^{-1} k^{-1}, $\Delta_r S^0_{m,2}(NpO_2(Ac)_2^-)$ = 89 ± 16 J mol^{-1} K^{-1}).[15] The formation of $NpO_2(Prop)$ is also endothermic with $\Delta_r H^0_m(NpO_2(Prop))$ = 10.9 ± 1.2 kJ mol^{-1} and $\Delta_r S^0_m(NpO_2(Prop))$ = 62 ± 4 J mol^{-1} K^{-1}.[16] This deviates from the observed thermodynamic behavior of the Np(V) formate complexation, where the formation of $NpO_2(Form)$ is slightly exothermic. In general, the formation of the Np(V) formate complexes has the lowest $\Delta_r H^0_{m,n}$ values compared with the respective acetate and propionate complex species.

Furthermore, the stoichiometric sum of the binary ion−ion interaction coefficients ($\Delta\varepsilon_{01}$ and $\Delta\varepsilon_{02}$) of the complexation reactions are obtained from SIT modeling according to eq 3. The calculated $\Delta\varepsilon_{01}$ and $\Delta\varepsilon_{02}$ values in $NaClO_4$ and NaCl media for the complexation reaction $NpO_2^+ + n\text{Form}^- \rightleftharpoons NpO_2(Form)_n^{1-n}$ (n = 1, 2) are displayed in Figure 7 as a function of the temperature. No temperature dependence of the $\Delta\varepsilon_{0n}$ values is observed, and averaged temperature independent $\Delta\varepsilon_{j,k}$ values are determined (see Table 2). This is in good agreement with results described in the literature on the ionic strength dependence of the complexation of Np(V) as well as trivalent lanthanides and actinides with various organic and inorganic ligands, where also no distinct effects of the temperature on $\Delta\varepsilon_{0n}$ were observed.[15,16,38,52−54] The averaged values are $\Delta\varepsilon_{01}$ = −0.09 ± 0.04 ($NaClO_4$), $\Delta\varepsilon_{01}$ = −0.10 ± 0.05 (NaCl), $\Delta\varepsilon_{02}$ = −0.16 ± 0.05 ($NaClO_4$) and $\Delta\varepsilon_{02}$ = −0.15 ± 0.06 (NaCl). The binary ion−ion interaction coefficients $\varepsilon_{j,k}$ of the different Np(V) formate complexes with Na^+ are calculated according to the SIT using equation 6 and the parameters: $\varepsilon(Na^+, Form^-)$ = 0.03 ± 0.01, $\varepsilon(NpO_2^+, ClO_4^-)$ = 0.25 ± 0.05, and $\varepsilon(NpO_2^+, Cl^-)$ = 0.09 ± 0.05 given by the NEA TDB.[49]

$$\Delta\varepsilon = \sum \varepsilon_{products} - \sum \varepsilon_{educt} \qquad (6)$$

The obtained results are $\varepsilon(Na^+ + Cl^-, NpO_2(Form))$ = 0.02 ± 0.07, $\varepsilon(Na^+ + ClO_4^-, NpO_2(Form))$ = 0.19 ± 0.06, $\varepsilon(Na^+, NpO_2(Form)_2^-)$ = −0.10 ± 0.09 for NaCl and $\varepsilon(Na^+, NpO_2(Form)_2^-)$ = 0.06 ± 0.08 for $NaClO_4$ as background electrolyte. The determined coefficients for both complex species differ by about 0.16 in NaCl and $NaClO_4$ media. Furthermore, the assumption of $\varepsilon_{i,k}$ = 0 for an uncharged species according to the SIT is not fulfilled for $\varepsilon(Na^+ + ClO_4^-, NpO_2(Form))$. In NaCl medium, $\varepsilon(Na^+ + Cl^-, NpO_2(Form))$ is in excellent accordance to zero.

Regarding the fact, that in NaCl solution a reasonable $\varepsilon_{j,k}$ value for the neutral $NpO_2(Form)$ complex is obtained, it is assumed that $\varepsilon(NpO_2^+, ClO_4^-)$ = 0.25 ± 0.05 reported in the NEA TDB is incorrect.[49] This assumption is supported by the fact that similar deviations were observed for the complexation of Np(V) with acetate and fluoride.[15,54] Nonetheless, in the present work the obtained log $\beta^0_n(T)$ values and thermody

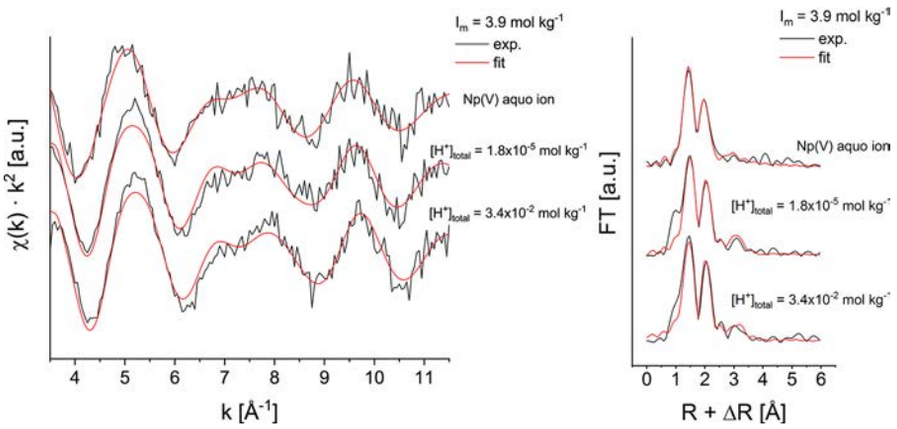

Figure 8. Raw k^2 weighted Np L_3 edge EXAFS spectra (left) and related Fourier transforms (right) of Np(V) in the presence of formate as a function of $[H^+]_{total}$ (black) and best fit from EXAFSPAK (red).

Table 5. Fit Parameters of the Raw k^2 Weighted Np L_3 Edge EXAFS Spectra Shown in Figure 8

$[H^+]_{total}$ [mol kg^{-1}]		1.8×10^{-5}	3.4×10^{-2}	Np(V) aquo ion
O_{ax}	N	2[a]	2[a]	2[a]
	R/Å	1.85(1)	1.83(1)	1.82(1)
	σ^2/Å^2	0.0008(4)	0.0006(4)	0.0002(3)
O_{mul}	N	4[a]	4[a]	4[a]
	R/Å	3.70[b]	3.66[b]	3.64[b]
	σ^2/Å^2	0.0017[b]	0.0014[b]	0.0005[b]
O_{eq}	N	3.0(4)	3.1(3)	5.1(6)
	R/Å	2.49(2)	2.47(2)	2.49(1)
	σ^2/Å^2	0.002(1)	0.001(1)	0.008(2)
C_c	N	2.0(9)	1.0(9)	
	R/Å	3.44(12)	3.32(6)	
	σ^2/Å^2	0.003*	0.003*	
species distribution	NpO_2(aq)	8%	19%	100%
	$NpO_2(Form)_2^-$	42%	50%	0%
	$NpO_2(Form)_2^-$	50%	29%	0%
expected C_c number from species distribution		1.4	1.1	0
ΔE_0/eV		18.2(5)	18.2(4)	7.2(6)
red. error with C shell		0.0292352	0.0261014	
red. error without C shell		0.0298219	0.0267350	0.0201802

[a]Parameter fixed. [b]Parameter depending on $X(O_{ax})$: $X(O_{mul}) = 2X(O_{ax})$. O_{ax} = axial O atoms, O_{mul} = multi scattering path of axial O atoms, O_{eq} = equatorial O atoms, and C_c = C atoms of coordinating COO^- groups.

namic functions determined in both electrolytes are in excellent agreement. This confirms that the ionic strength dependency of the complex formation is accurately described in both background electrolytes using the here determined $\Delta\varepsilon_{0,n}$ values.

A comparison with literature data is not possible due to the lack of data on the ionic strength dependence of the Np(V) complexation with formate.

3.5. EXAFS Spectroscopy. The complex geometry and coordination mode of formate toward the metal ion are studied by EXAFS spectroscopy at a fixed ligand concentration ($[Form^-]_{total}$ = 0.6 mol kg^{-1}) as a function of the total proton concentration ($[H^+]_{total}$ = 1.8×10^{-5}, 3.4×10^{-2} mol kg^{-1}). Varying proton concentration affects the species distribution of the Np(V) formate complexes as $[Form^-]_{eq}$ changes. Additionally, effects of the proton concentration on the coordination mode of formate toward the metal center can simultaneously be investigated. The calculated species distribution of the formed complexes as a function of $[H^+]_{total}$ is given in the Supporting Information (Figure S2). Additionally, the Vis/NIR absorption spectra of the EXAFS sample solutions are displayed in Figure S3. Absorption spectroscopic measurements of the EXAFS samples before and after irradiation by the X ray beam confirms that no redox processes occurred during EXAFS measurements.

The experimentally obtained k^2 weighted Np L_3 edge EXAFS spectra of Np(V) in the presence of formate, their Fourier transformations and the corresponding fit curves are displayed in Figure 8 for two different pH_c values. The deconvolution of the fit cures is given in Figures S4 and S5 in the Supporting Information. The results of the fits and the fit parameters are listed in Table 5 with the calculated speciation at the given experimental conditions. The spectra are dominated by the axial and equatorial O atoms (O_{ax}, O_{eq}) at a distance of O_{ax} = 1.84 ± 0.02 Å and O_{eq}= 2.48 ± 0.05 Å. These values are in excellent agreement with literature data (O_{ax} = 1.81−1.85 Å; O_{eq} = 2.47−2.54).[16,17,55] In order to determine the coordination mode of formate toward the metal center the distance of the carboxylic carbon atom (C_c) has to be taken into account. The results show an averaged distance

of the C_c atom of 3.38 ± 0.10 Å. Takao et al. studied the complexation of Np(V) with acetate by EXAFS spectroscopy.[17] They determined a C_c distance of 2.91 ± 0.02 Å between the Np(V) center and the C atom of the coordinating COO^- group. Vasiliev et al. investigated the complexation of Np(V) with propionate.[16] There, the C_c distance was 2.87 ± 0.03 Å. Both ligands coordinate bidentate to the metal ion via both O atoms of the COO^- group. Thus, these distances serve as references for a bidentate coordination of the COO^- group. The C_c distance of the $NpO_2(Form)_n^{1-n}$ complexes are approximately 0.5 Å longer compared to the literature values for the acetate and propionate species. This indicates that in the case of formate the COO^- group coordinates in a monodentate mode via only one oxygen atom toward the Np(V) center. This result is in excellent agreement with EXAFS studies by Fröhlich et al. concerning the complexation of Am(III) with formate.[56] There, a C_c distance of 3.40 ± 0.02 Å was determined, which was attributed to a monodentate coordination of formate via only one O atom toward the Am(III). The determined distance between the Am(III) ion and the O atoms of the coordinating formate was determined as O_c = 2.409 ± 0.007 Å. This value is also in excellent agreement with the distances of the equatorial O atoms to the Np(V) center (O_{eq} = 2.48 ± 0.05 Å) in the present work. These results show that the bond distance and coordination mode of formate toward the metal center is equal for An(III) and An(V) ions.

The differences in the coordination modes of formate compared with acetate and propionate explains the observed differences in the thermodynamic functions and complex stabilities. The monodentate coordination of formate is expected to be weaker compared to the bidentate binding of acetate and propionate which is represented by higher log β^0_n values of $NpO_2(Ac)_n^{1-n}$ and $NpO_2(Prop)_n^{1-n}$ compared with $NpO_2(Form)_n^{1-n}$. Furthermore, the Np(V) formate complexes have a free noncoordinating O atom of the ligand enabling the formation of hydrogen bonds with the second coordination sphere (water shell). Thus, the solvation enthalpies of the Np(V) formate complexes are lower which results in lower $\Delta_r H^0_{m,n}$ values.

3.6. Quantum Chemical Calculations. The molecular structures of the $NpO_2(Form)$ and $NpO_2(Form)_2^-$ complexes with mono and bidentate coordinating formate molecules (see Figure 9) are optimized on DFT level using the BH LYP functional and the def TZVP basis sets. All probed structures are given in more detail in Figures S6 and S7 in the Supporting Information. The calculated bond distances are summarized in Table 6 and compared to the EXAFS results. The results show that the calculated distances of the axial (O_{ax}) and equatorial O atoms (O_{eq}) are independent of the coordination mode of the ligand molecules. However, the distance of the carboxylic C atom increases from bidentate to monodentate coordination. The calculated C_c distance for monodentate binding is about 0.4 Å longer compared to bidentate binding. A comparison with the EXAFS results reveals that the experimentally obtained distances of the O and C atoms are in excellent agreement with the quantum chemically calculations for the monodentate coordination mode and confirms the coordination by only one O atom of the COO^- group of formate toward the Np(V) ion.

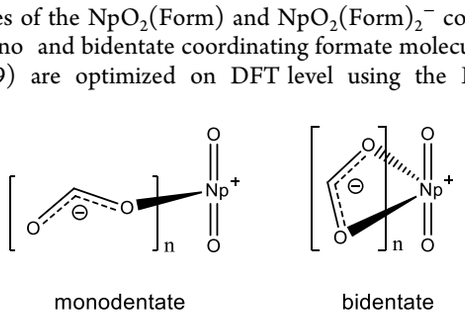

Figure 9. Schematic structures of the optimized Np(V) formate complexes (n = 1, 2). Water molecules are omitted for clarity.

Calculations of the Gibbs free energies ΔG for the isomerization reactions according to eq 7 also confirm the monodentate coordination of formate toward Np(V).

$$NpO_2(Form)_{(bidentate)} \rightleftharpoons NpO_2(Form)_{(monodentate)}$$
$$NpO_2(Form)_2^-{}_{(bidentate)} \rightleftharpoons NpO_2(Form)_2^-{}_{(monodentate)} \quad (7)$$

The ΔG values for these isomerization reactions are calculated using the difference of the ground state energies ΔE_g on MP2 level taking into account thermodynamic corrections ΔE_{vib} and solvation effects ΔE_{solv}: $\Delta G = \Delta E_g + \Delta E_{vib} + \Delta E_{solv}$ ($\Delta E = E_{monodentate} - E_{bidentate}$). The results are listed in Table 7. The calculated ΔG values are negative for both complex species. This confirms that the monodentate coordination is energetically more stable than the bidentate coordination.

4. SUMMARY AND CONCLUSION

In the present work, the thermodynamics of the complexes of Np(V) with formate are studied systematically as a function of the ligand concentration ($[Form^-]_{total}$), ionic strength (NaCl and $NaClO_4$), and temperature (20−85 °C) using absorption spectroscopy. Under the experimental conditions, the formation of two different complex species is observed which are identified as $NpO_2(Form)$ and $NpO_2(Form)_2^-$ by principle component analyses and slope analyses. With increasing temperature, the formation of the 1:1 complex is slightly repressed which is reflected by a decrease of log $\beta^0_1(T)$ of 0.1 logarithmic units. In contrast, the formation of the 1:2 complex is more pronounced at elevated temperatures with an increase of the thermodynamic stability constant by 0.2. Correlation of log $\beta^0_n(T)$ with the reciprocal temperature and fitting according to the integrated Van't Hoff equation yield the standard reaction enthalpies ($\Delta_r H^0_{m,n}$) and entropies ($\Delta_r S^0_{m,n}$) of the complexation reactions. The results show that the first complexation step is slightly exothermic whereas the formation of $NpO_2(Form)_2^-$ is endothermic.

Furthermore, the stoichiometric sum of the SIT specific binary ion−ion interaction coefficients, $\Delta\varepsilon_{01}$ and $\Delta\varepsilon_{02}$, are determined as a function of temperature for two different ionic media (NaCl and $NaClO_4$ solutions). As a result, no significant temperature dependence of $\Delta\varepsilon_{01}$ and $\Delta\varepsilon_{02}$ is observed.

Structural investigations of the formed complexes by EXAFS spectroscopy and quantum chemical calculations reveal a monodentate coordination of formate toward the Np(V) ion highlighting the effect of the alkyl chain in monocarboxylates on the binding mode of the ligands toward the metal center.

The present work provides a detailed description of the complexation of Np(V) with formate on a molecular level. The here determined structural and thermodynamic data are a valuable contribution to the thermodynamic database of actinides improving the scientific basis for describing the chemical behavior of pentavalent actinides in natural aquatic systems in the presence of small organic ligands.

Table 6. Distances of the Ligand Atoms and the Metal Center and Comparison of the Experimental Results and Quantum Chemical Calculations

method	complex	coord. mod.	O_{ax} [Å]	O_{eq} [Å]	C_c [Å]
DFT	$NpO_2(Form)$	monodentate	1.82	2.47	3.38
		bidentate	1.81	2.50	2.94
	$NpO_2(Form)_2^-$	monodentate	1.83	2.47	3.34
		bidentate	1.80	2.54	2.93
EXAFS	$NpO_2(Form)/NpO_2(Form)_2^-$		1.84 ± 0.01	2.48 ± 0.03	3.38 ± 0.10

Table 7. Gibbs Free Energies for the Isomerization Reactions According to eq 7[a]

complex	ΔE_g [kJ mol^{-1}]	ΔE_{vib} [kJ mol^{-1}]	ΔE_{solv} [kJ mol^{-1}]	ΔG [kJ mol^{-1}]
$NpO_2(Form)$	1.184	14.401	13.785	29.370
$NpO_2(Form)_2^-$	12.206	7.218	38.080	33.092

[a]Ground state energies E_g were calculated on the MP2 level.

AUTHOR INFORMATION

Corresponding Author

Martin M. Maiwald − *Physikalisch Chemisches Institut, Ruprecht Karls Universität Heidelberg, D 69120 Heidelberg, Germany;* orcid.org/0000 0003 3137 6214; Email: m.maiwald@pci.uni heidelberg.de

Authors

Kathy Dardenne − *Institut für Nukleare Entsorgung (INE), Karlsruher Institut für Technologie (KIT), D 76344 Eggenstein Leopoldshafen, Germany*

Jörg Rothe − *Institut für Nukleare Entsorgung (INE), Karlsruher Institut für Technologie (KIT), D 76344 Eggenstein Leopoldshafen, Germany*

Andrej Skerencak Frech − *Institut für Nukleare Entsorgung (INE), Karlsruher Institut für Technologie (KIT), D 76344 Eggenstein Leopoldshafen, Germany;* orcid.org/0000 0003 2177 4462

Petra J. Panak − *Physikalisch Chemisches Institut, Ruprecht Karls Universität Heidelberg, D 69120 Heidelberg, Germany; Institut für Nukleare Entsorgung (INE), Karlsruher Institut für Technologie (KIT), D 76344 Eggenstein Leopoldshafen, Germany*

Notes

The authors declare no competing financial interest.

ACKNOWLEDGMENTS

All spectroscopic measurements were carried out at the Institute for Nuclear Waste Disposal (INE) at Karlsruhe Institute of Technology (KIT). Dr. D. Fellhauer and Dr. M Altmaier are acknowledged for providing the ^{237}Np and their experimental support. This work is supported by the German Federal Ministry of Education and Research (BMBF) under Contract 02NUK039C.

REFERENCES

(1) Geckeis, H.; Röhlig, K. J.; Mengel, K. Endlagerung radioaktiver Abfälle. *Chem. Unserer Zeit* **2012**, *46* (5), 282−293.

(2) OECD; Agency, N. E.. *Considering Timescales in the Post closure Safety of Geological Disposal of Radioactive Waste* **2009**, DOI: 10.1787/9789264060593 en.

(3) Geckeis, H.; Lutzenkirchen, J.; Polly, R.; Rabung, T.; Schmidt, M. Mineral water interface reactions of actinides. *Chem. Rev.* **2013**, *113* (2), 1016−62.

(4) Runde, W. The chemical interactions of actinides in the environment. *Los Alamos Science* **2000**, *26*, 392−411.

(5) Choppin, G. R. Actinide speciation in the environment. *J. Radioanal. Nucl. Chem.* **2007**, *273* (3), 695−703.

(6) Choppin, G. R. Actinide speciation in aquatic systems. *Mar. Chem.* **2006**, *99* (1−4), 83−92.

(7) Gens, R.; Lalieux, P.; Preter, P. D.; Dierckx, A.; Bel, J.; Boyazis, J. P.; Cool, W. The Second Safety Assessment and Feasibility Interim Report (SAFIR 2 Report) on HLW Disposal in Boom Clay: Overview of the Belgian Programme. *MRS Proceedings* **2003**, *807*, 917−924.

(8) Oecd, N. E. A. *Safety of Geological Disposal of High level and Long lived Radioactive Waste in France*; Nuclear Energy Agency Organisation for Economic Co Operation and Development: 2006.

(9) Hoth, P.; Wirth, H.; Reinhold, K.; Bräuer, V.; Krull, P.; Feldrappe, H. *Endlagerung radioaktiver Abfälle in tiefen geologischen Formationen Deutschlands Untersuchung und Bewertung von Tonges teinsformationen*. BGR Bundesanstalt für Geowissenschaften und Rohstoffe: Hannover, Germany, 2007.

(10) NAGRA *Projekt Opalinuston Synthese der geowissenschaftlichen Untersuchungsergebnisse, Entsorgungsnachweis für abgebrannte Brennele mente, verglaste hochaktive sowie langlebige mittelaktive Abfälle*; NAGRA Nationale Genossenschaft für die Lagerung radioaktiver Abfälle: Wettingen, Switzerland, 2002.

(11) Gaucher, E.; Robelin, C.; Matray, J.; Negrel, G.; Gros, Y.; Heitz, J.; Vinsot, A.; Rebours, H.; Cassagnabere, A.; Bouchet, A. ANDRA underground research laboratory: interpretation of the mineralogical and geochemical data acquired in the Callovian Oxfordian formation by investigative drilling. *Physics and Chemistry of the Earth, Parts A/B/C* **2004**, *29* (1), 55−77.

(12) Allen, T. R.; Stoller, R. E.; Yamanaka, S. *Comprehensive Nuclear Materials*. Elsevier: Amsterdam, The Netherlands, 2012.

(13) Courdouan, A.; Christl, I.; Meylan, S.; Wersin, P.; Kretzschmar, R. Isolation and characterization of dissolved organic matter from the Callovo Oxfordian formation. *Appl. Geochem.* **2007**, *22* (7), 1537−1548.

(14) Courdouan, A.; Christl, I.; Meylan, S.; Wersin, P.; Kretzschmar, R. Characterization of dissolved organic matter in anoxic rock extracts and in situ pore water of the Opalinus Clay. *Appl. Geochem.* **2007**, *22* (12), 2926−2939.

(15) Maiwald, M. M.; Skerencak Frech, A.; Panak, P. J. The complexation and thermodynamics of neptunium(V) with acetate in aqueous solution. *New J. Chem.* **2018**, *42* (10), 7796−7802.

(16) Vasiliev, A. N.; Banik, N. L.; Marsac, R.; Froehlich, D. R.; Rothe, J.; Kalmykov, S. N.; Marquardt, C. M. Np(v) complexation with propionate in 0.5−4 M NaCl solutions at 20−85 degrees C. *Dalton Trans* **2015**, *44* (8), 3837−44.

(17) Takao, K.; Takao, S.; Scheinost, A. C.; Bernhard, G.; Hennig, C. Complex formation and molecular structure of neptunyl(VI) and (V) acetates. *Inorg. Chem.* **2009**, *48* (18), 8803−10.
(18) Rao, L.; Tian, G.; Srinivasan, T. G.; Zanonato, P.; Di Bernardo, P. Spectrophotometric and Calorimetric Studies of Np(V) Complex ation with Acetate at Various Temperatures from T = 283 to 343 K. *J. Solution Chem.* **2010**, *39* (12), 1888−1897.
(19) Pokrovsky, O. S.; Choppin, G. R. Neptunium(V) Complexation by Acetate, Oxalate and Citrate in NaClO4Media at 25°C. *Radiochim. Acta* **1997**, *79* (3), 167−171.
(20) Moore, R. C.; Borkowski, M.; Bronikowski, M. G.; Chen, J.; Pokrovsky, O. S.; Xia, Y.; Choppin, G. R. Thermodynamic Modeling of Actinide Complexation with Acetate and Lactate at High Ionic Strength. *J. Solution Chem.* **1999**, *28* (5), 521−531.
(21) Fellhauer, D.; Rothe, J.; Altmaier, M.; Neck, V.; Runke, J.; Wiss, T.; Fanghänel, T. Np(V) solubility, speciation and solid phase formation in alkaline CaCl2 solutions. Part I: Experimental results. *Radiochim. Acta* **2016**, *104* (6), 355−379.
(22) Tasi, A.; Gaona, X.; Fellhauer, D.; Bottle, M.; Rothe, J.; Dardenne, K.; Schild, D.; Grive, M.; Colas, E.; Bruno, J.; Kallstrom, K.; Altmaier, M.; Geckeis, H. Redox behavior and solubility of plutonium under alkaline, reducing conditions. *Radiochim. Acta* **2018**, *106* (4), 259−279.
(23) Denecke, M. A.; Rothe, J.; Dardenne, K.; Blank, H.; Hormes, J. The INEBeamline for Actinide Research at ANKA. *Phys. Scr.* **2005**, 1001.
(24) Rothe, J.; Butorin, S.; Dardenne, K.; Denecke, M. A.; Kienzler, B.; Loble, M.; Metz, V.; Seibert, A.; Steppert, M.; Vitova, T.; Walther, C.; Geckeis, H. The INE Beamline for actinide science at ANKA. *Rev. Sci. Instrum.* **2012**, *83* (4), 043105.
(25) Rothe, J.; Denecke, M. A.; Dardenne, K.; Fanghänel, T., The INE Beamline for actinide research at ANKA. *Radiochim. Acta* **2006**, *94* (9−11).691
(26) Newville, M. IFEFFIT: interactive XAFS analysis and FEFFfitting. *J. Synchrotron Radiat.* **2001**, *8* (2), 322−324.
(27) George, G. N.; Pickering, I. J., *EXAFSPAK: A suite of computer programs for analysis of X ray absorption spectra*; SSRL, Stanford: 1995.
(28) Ravel, B.; Newville, M. ATHENA, ARTEMIS, HEPHAESTUS: data analysis for X ray absorption spectroscopy using IFEFFIT. *J. Synchrotron Radiat.* **2005**, *12* (4), 537−541.
(29) Rehr, J. J.; Kas, J. J.; Prange, M. P.; Sorini, A. P.; Takimoto, Y.; Vila, F. Ab initio theory and calculations of X ray spectra. *C. R. Phys.* **2009**, *10* (6), 548−559.
(30) Bombieri, G.; Benetollo, F.; Del Pra, A.; Rojas, R. Structural studies on the actinide carboxylates—IV The crystal and molecular structure of succinate dioxouranium(VI) monohydrate. *J. Inorg. Nucl. Chem.* **1979**, *41* (2), 201−203.
(31) Lermontov, A. S.; Lermontova, E. K.; Wang, Y. Y. Synthesis, structure and optic properties of 2 methylimidazolium and 2 phenylimidazolium uranyl acetates. *Inorg. Chim. Acta* **2009**, *362* (10), 3751−3755.
(32) Furche, F.; Ahlrichs, R.; Hättig, C.; Klopper, W.; Sierka, M.; Weigend, F. Turbomole. *Wiley Interdiscip. Rev.: Comput. Mol. Sci.* **2014**, *4* (2), 91−100.
(33) Becke, A. D. A new mixing of Hartree Fock and local density functional theories. *J. Chem. Phys.* **1993**, *98* (2), 1372.
(34) Küchle, W.; Dolg, M.; Stoll, H.; Preuss, H. Energy adjusted pseudopotentials for the actinides. Parameter sets and test calculations for thorium and thorium monoxide. *J. Chem. Phys.* **1994**, *100* (10), 7535.
(35) Weigend, F.; Häser, M. RI MP2: first derivatives and global consistency. *Theor. Chem. Acc.* **1997**, *97* (1−4), 331−340.
(36) Weigend, F.; Häser, M.; Patzelt, H.; Ahlrichs, R. RI MP2: optimized auxiliary basis sets and demonstration of efficiency. *Chem. Phys. Lett.* **1998**, *294* (1−3), 143−152.
(37) Klamt, A.; Schüürmann, G. COSMO: a new approach to dielectric screening in solvents with explicit expressions for the screening energy and its gradient. *J. Chem. Soc., Perkin Trans. 2* **1993**, *2* (5), 799.
(38) Maiwald, M. M.; Sittel, T.; Fellhauer, D.; Skerencak Frech, A.; Panak, P. J. Thermodynamics of neptunium(V) complexation with sulfate in aqueous solution. *J. Chem. Thermodyn.* **2018**, *116*, 309−315.
(39) Hagan, P. G.; Cleveland, J. M. The absorption spectra of neptunium ions in perchloric acid solution. *J. Inorg. Nucl. Chem.* **1966**, *28* (12), 2905−2909.
(40) Friedman, H. A.; Toth, L. M. Absorption spectra of Np(III), (IV), (V) and (VI) in nitric acid solution. *J. Inorg. Nucl. Chem.* **1980**, *42* (9), 1347−1349.
(41) Yang, Y.; Zhang, Z.; Liu, G.; Luo, S.; Rao, L. Effect of temperature on the complexation of NpO 2 + with benzoic acid: Spectrophotometric and calorimetric studies. *J. Chem. Thermodyn.* **2015**, *80*, 73−78.
(42) Zhang, Z.; Yang, Y.; Liu, G.; Luo, S.; Rao, L. Effect of temperature on the thermodynamic and spectroscopic properties of Np(v) complexes with picolinate. *RSC Adv.* **2015**, *5* (92), 75483−75490.
(43) Skerencak, A.; Panak, P. J.; Hauser, W.; Neck, V.; Klenze, R.; Lindqvist Reis, P.; Fanghanel, T. TRLFS study on the complexation of Cm(III) with nitrate in the temperature range from 5 to 200 degrees C. *Radiochim. Acta* **2009**, *97* (8), 385−393.
(44) Neck, V.; Fanghänel, T.; Rudolph, G.; Kim, J. I. Thermodynamics of Neptunium(Y) in Concentrated Salt Solutions: Chloride Complexation and Ion Interaction (Pitzer) Parameters for the NpO+2 Ion. *Radiochim. Acta* **1995**, *69* (1), 39−47.
(45) Skerencak, A.; Panak, P. J.; Fanghänel, T. Complexation and thermodynamics of Cm(III) at high temperatures: the formation of $[Cm(SO_4)_n]^{3-2n}$ (n = 1, 2, 3) complexes at T = 25 to 200°C. *Dalton Trans.* **2013**, *42*, 542−549.
(46) Fröhlich, D. R.; Skerencak Frech, A.; Panak, P. J. Complex formation of Cm(III) with formate studied by time resolved laser fluorescence spectroscopy. *Appl. Geochem.* **2015**, *61*, 312−317.
(47) Hummel, W.; Puigdomenech, I.; Rao, L.; Tochiyama, O. Thermodynamic data of compounds and complexes of U, Np, Pu and Am with selected organic ligands. *C. R. Chim.* **2007**, *10*, 948−958.
(48) Motekaitis, R. J.; Martell, A. E.; Smith, R. M. *NIST Critically Selected Stability Constants of Metal Complexes. NIST Standard Reference Database 46*, version 6; U.S. Department of Commerce, Technology Administration, National Institute of Standards and Technology, Standard Reference Data Program: Gaithersburg, MD, 2001.
(49) Guillaumont, R.; Fanghänel, T.; Neck, V.; Fuger, J.; Palmer, D. A. *Update on the Chemical Thermodynamics of Uranium, Neptunium, Plutonium, Americium and Technetium*; Elsvier B.V.: 2003.
(50) Lemire, R. J. *Chemical thermodynamics of neptunium and plutonium*; Elsevier: 2001; Vol. *4*.
(51) Novak, C. F.; Borkowski, M.; Choppin, G. R. Thermodynamic Modeling of Neptunium(V) Acetate Complexation in Concentrated NaCl Media. *Radiochim. Acta* **1996**, *74* (s1), 111−116.
(52) Fröhlich, D. R.; Skerencak Frech, A.; Panak, P. J. A spectroscopic study on the formation of Cm(III) acetate complexes at elevated temperatures. *Dalton Trans* **2014**, *43* (10), 3958−65.
(53) Skerencak Frech, A.; Maiwald, M.; Trumm, M.; Froehlich, D. R.; Panak, P. J. The complexation of Cm(III) with oxalate in aqueous solution at T = 20−90 degrees C: a combined TRLFS and quantum chemical study. *Inorg. Chem.* **2015**, *54* (4), 1860−8.
(54) Maiwald, M. M.; Fellhauer, D.; Skerencak Frech, A.; Panak, P. J. The complexation of neptunium(V) with fluoride at elevated temperatures: Speciation and thermodynamics. *Appl. Geochem.* **2019**, *104*, 10−18.
(55) Allen, P. G.; Bucher, J. J.; Shuh, D. K.; Edelstein, N. M.; Reich, T. Investigation of Aquo and Chloro Complexes of UO22+, NpO2+, Np4+, and Pu3+by X ray Absorption Fine Structure Spectroscopy. *Inorg. Chem.* **1997**, *36* (21), 4676−4683.
(56) Fröhlich, D. R.; Kremleva, A.; Rossberg, A.; Skerencak Frech, A.; Koke, C.; Krüger, S.; Rosch, N.; Panak, P. J. Combined EXAFS Spectroscopic and Quantum Chemical Study on the Complex Formation of Am(III) with Formate. *Inorg. Chem.* **2017**, *56* (12), 6820−6829.